Research Article

Nadezhda K. Pavlycheva and Eduard R. Muslimov*

Compact dual-band spectrograph

Abstract: A concept and design method of a dual-band flat-field spectrograph is presented. In the proposed optical scheme, the working range of wavelengths is divided into two subranges. A reflection holographic grating is used in the first subrange, and a transmission concave holographic grating is used in the second one. Both of them are aberration-corrected flat-field gratings. As an example, a scheme of spectrograph for spectral range from 278 to 560 nm is considered.

Keywords: aberration correction; flat-field spectrograph; transmission concave holographic grating.

OCIS codes: 120.6200; 050.1950; 090.2890.

***Corresponding author: Eduard R. Muslimov,** Kazan National Research Technical University, Department of Optical and Electronic Systems, 10 K. Marks str, Kazan, Tatarstan 420111, Russian Federation, e-mail: eduard.r.muslimov@gmail.com
Nadezhda K. Pavlycheva: Kazan National Research Technical University, Department of Optical and Electronic Systems, Kazan, Tatarstan, Russian Federation

1 Introduction

At present, optical schemes of flat-field spectrographs on the basis of nonclassical concave diffraction gratings are widely used in spectral devices. The obvious advantages of such schemes include simple and compact design, comparatively high resolution and throughput, as well as an absence of moving parts. Nowadays, there are numerous commercial spectrometers for such applications as metal and alloy analysis, atmosphere analysis, tissue and biological media investigation, etc., based on these schemes [1–3]. On the other hand, the flat-field spectrograph schemes are constantly improved. The main trends of the enhancement are expansion of the working spectral range, increase of the spectral resolution and throughput, as well as the reduction of overall size of the device [4–7].

In the present work, we propose a concept and design procedure of a dual-band flat-field spectrograph with reflection and transmission concave holographic diffraction gratings. Such spectrograph is notable for its extended wavelength range and moderate high resolution. In the next section, a theoretical basis of the design method is provided. Further, examples of the design and modeling of the channels for UV and visible spectra are presented, respectively. The last section contains the general conclusions on the research.

2 Theoretical description

The main idea of the proposed optical scheme is dividing of the working spectral range into two simultaneously detected subranges. Each of the subranges is registered by a separate channel of the device representing a flat-field spectrograph with concave holographic diffraction grating. A reflection holographic grating is used in the first channel; the second channel is based on a transmission holographic diffraction grating mounted in a converging beam formed in the zero order of diffraction of the first channel. In such a layout, image of the entrance slit of the device generated in the zero order of diffraction serves as a virtual slit of the second channel. This approach provides a high spectral resolution in the extended range of wavelengths and does not require an increase of the scheme dimensions.

Our design procedure of the flat-field spectrographs schemes is based on a separate term minimization of the holographic grating aberration function. It enables an analytical definition of the scheme parameters and the grating recording parameters, which provide correction of defocusing, astigmatism, and meridional coma on a plane perpendicular to the ray of the average wavelength diffracted by the grating vertex.

The design method of a flat-field spectrograph based on a reflection holographic grating is stated, for example, in [8]. It was shown that the method assures a good aberration correction in a relatively small spectral range. For the proposed design, we use the mentioned procedure without any changes. The only distinction from the

general procedure consists of the limitation of the angle of incidence introduced in order to constrain the astigmatism in the zero order of diffraction.

The design algorithm of the flat-field spectrograph with a transmission concave holographic grating also relies on the analysis of the grating aberration function. A combined scheme of the recording and work of the transmission concave holographic grating is shown in Figure 1. The Cartesian coordinate system of the grating is defined as follows: origin O is in the grating vertex, the X axis is normal to the grating surface, and the Z axis is directed along the grooves. Other designations on the scheme are A – point on the entrance slit; A' – its image; O_1 and O_2 – point sources of recording radiation; φ, φ' – angles of incidence and diffraction, respectively; d, d' – distance from the grating vertex to points A and A', respectively, (i_1, d_1) and (i_2, d_2) – polar coordinates in the XY plane of the recording sources O_1 and O_2, respectively.

The optical path function for the beam emitted from the center of the entrance slit and diffracted at an arbitrary point of the grating surface $M(x, y, z)$, is given by

$$V=(AM)+(MA')-k\lambda m(y, z), \tag{1}$$

where k is the order of diffraction, λ is the wavelength, and $m(y, z)$ is the number of grooves on the grating surface between the grating vertex O and the point M. After substituting of the equation of the spherical grating surface with the radius of curvature equal to R, the expansion into series, and the grouping of terms, we obtain a concave transmission grating aberration function in following form:

$$\begin{aligned} V=&-yF_0+\frac{y^2}{2R}F_1+\frac{z^2}{2R}F_2+\frac{y^3}{2R^2}F_3+\frac{yz^2}{2R^2}F_4\\ &+\frac{y^4}{8R^3}F_5+\frac{y^2z^2}{4R^3}F_6+\frac{z^4}{8R^3}F_7+\cdots \end{aligned} \tag{2}$$

The coefficients F_i are expressed in the form

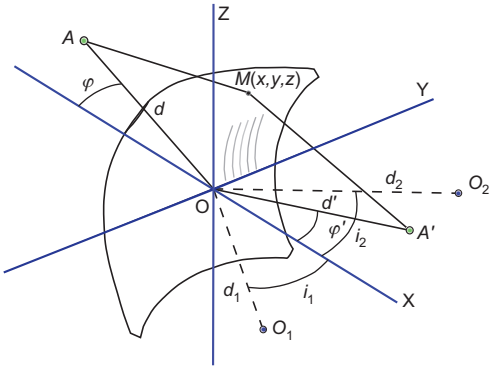

Figure 1 Combined scheme of the recording and work of a transmission holographic diffraction grating.

$$F_i=M_i-\frac{k\lambda}{\lambda_0}H_i, \tag{3}$$

where the coefficient M_i contains the scheme parameters, H_i contains the recording parameters, λ is the working wavelength, and λ_0 is the recording wavelength.

Condition $F_0=0$ gives us the transmission grating equation. Coefficient F_1 characterizes the beam focusing in the meridional plane XY, F_2 characterizes the beam focusing in the sagittal plane XZ and consequently the astigmatism, F_3 determines the meridional coma, F_4 determines the sagittal coma; and finally, F_5, F_6, and F_7 characterize the third-order aberrations. The condition of correction of a corresponding aberration is given by

$$F_i=0 \tag{4}$$

The first four coefficients of the expansion (2) are written as

$$F_0=-\sin\varphi+\sin\varphi'-\frac{k\lambda}{\lambda_0}(\sin i_1-\sin i_2), \tag{5}$$

$$F_1=R\left[\left(-\frac{\cos^2\varphi}{d}+\frac{\cos\varphi}{R}\right)+\left(\frac{\cos^2\varphi'}{d'}-\frac{\cos\varphi'}{R}\right)\right]-\frac{k\lambda}{\lambda_0}H_1, \tag{6}$$

$$F_2=R\left[\left(-\frac{1}{d}+\frac{\cos\varphi}{R}\right)+\left(\frac{1}{d'}-\frac{\cos\varphi'}{R}\right)\right]-\frac{k\lambda}{\lambda_0}H_2, \tag{7}$$

$$\begin{aligned} F_3=R^2\Bigg[&-\frac{\sin\varphi}{d}\left(-\frac{\cos^2\varphi}{d}+\frac{\cos\varphi}{R}\right)-\frac{\sin\varphi'}{d'}\\ &\left(\frac{\cos^2\varphi'}{d'}-\frac{\cos\varphi'}{R}\right)\Bigg]-\frac{k\lambda}{\lambda_0}H_3. \end{aligned} \tag{8}$$

It should be mentioned that the holographic coefficients H_i are identical for both of transmission and reflection concave holographic gratings [8, 9]:

$$H_1=\cos i_1\left(\frac{R}{d_1}\cos i_1-1\right)-\cos i_2\left(\frac{R}{d_2}\cos i_2-1\right), \tag{9}$$

$$H_2=\frac{R}{d_1}-\frac{R}{d_2}-\cos i_1+\cos i_2, \tag{10}$$

$$H_3=\sin i_1\cos i_2\frac{R}{d_1}\left(1-\cos i_1\frac{R}{d_1}\right)-\sin i_2\cos i_2\frac{R}{d_2}\left(1-\cos i_2\frac{R}{d_2}\right). \tag{11}$$

Further, we define the conditions of aberration correction on a plane. The spectrum plane is assumed to be perpendicular to the beam of the average wavelength λ_{av}

diffracted by the grating vertex to the diffraction angle ϕ'_{av}. Then, the distance from the vertex to the diffraction focus of a wavelength λ should be equal to

$$d' = \frac{d'_{av}}{\cos(\varphi'_{av} - \varphi')}. \quad (12)$$

The aberration correction is achieved by means of an appropriate choice of the distance from the grating vertex to the spectrum detection plane d'_{av} and the recording parameters of the grating. In our case, the condition of correction of the defocusing across the field (13) is defined with round-mean square technique. The conditions of correction of astigmatism (14) and meridional coma (15) are derived for the average wavelength λ_{av}. As a result, the conditions of aberration correction on a plane are determined by the following equations

$$\frac{\partial I_1}{\partial H_1} = 0, \quad \frac{\partial I_1}{\partial d'_{av}} = 0, \quad (13)$$

$$R\left(-\frac{1}{d} + \frac{\cos\varphi}{R}\right) + \left(\frac{1}{d'_{av}} - \frac{\cos\varphi'_{av}}{R}\right) - \frac{k\lambda_{av}}{\lambda_0} H_2 = 0, \quad (14)$$

$$R^2\left[-\frac{\sin\varphi}{d}\left(-\frac{\cos^2\varphi}{d} + \frac{\cos\varphi}{R}\right) + \frac{\sin\varphi'_{av}}{d'_{av}}\left(\frac{\cos^2\varphi'_{av}}{d'_{av}} - \frac{\cos\varphi'_{av}}{R}\right)\right] - \frac{k\lambda_{av}}{\lambda_0} H_3 = 0, \quad (15)$$

where

$$I_1 = \int_{\varphi'_1}^{\varphi'_2} F_1^2 d\varphi'. \quad (16)$$

We should take into account also the well-known relations for the holographic gratings:

$$\frac{\sin\varphi - \sin\varphi'}{\sin i_1 - \sin i_2} = \frac{k\lambda}{\lambda_0}; \quad \sin i_1 - \sin i_2 = N\lambda_0, \quad (17)$$

where N is the groove density in the grating vertex.

After successful integration, differentiation, and substitution of expressions (16) and (17) into Eqs (13)–(15), we obtain a system of linear equations, from which we can calculate the values of d'_{av} and H_1, H_2, H_3. Further, we can derive the recording sources coordinates (i_1,d_1) and (i_2, d_2) for a selected wavelength λ_0 from the expressions (9)–(11) defining H_i.

As an example of implementation of the proposed method, a scheme of the spectrograph for the spectral range from 278 to 560 nm is considered. The working spectral range is divided into two parts, namely, the first UV subrange stretching from 278 to 400 nm detected using a reflection holographic grating, and the second visible subrange from 400 to 560 nm, detecting with transmission holographic grating. The relative aperture of the optical system in this example is about 1/10, which is appropriate, for instance, for atomic emission analysis. Figure 2 represents a general view of the optical scheme of the dual-band spectrograph. Detailed description of the design and modeling of each of the channels is provided in the following sections. Both of the gratings have quasisinusoidal groove profile. Therefore, their diffraction efficiency is relatively low, but uniform in the working spectral range. This is acceptable for the applications that use powerful radiation sources, such as emission spectral analysis of metals and alloys. If a higher value of the diffraction efficiency is required, the gratings can be fabricated with the well-known ion-etching blazing technology.

3 Optical scheme of UV channel

The UV channel of the device operates in the spectral range of 278–400 nm. The channel is based on the reflection concave holographic grating. The grating radius of curvature is equal to 150 mm, the diameter is 15.6 mm, the groove density in the grating vertex is 1340 grooves per mm. The angle of incidence is 9°. As was proven by calculations, the aberrations of the reflection grating in the zero order of diffraction are negligible for this angle. The spectrum length is 27.3 mm, which corresponds to the length of the sensitive area of a commercial linear CCD detector, for example, Hamamatsu S9840 (Hamamatsu Photonics K.K., Hamamatsu City, Japan) [10]. The reciprocal linear dispersion of the channel is 4.47 nm/mm. The distance between the entrance slit and the grating vertex is 155 mm.

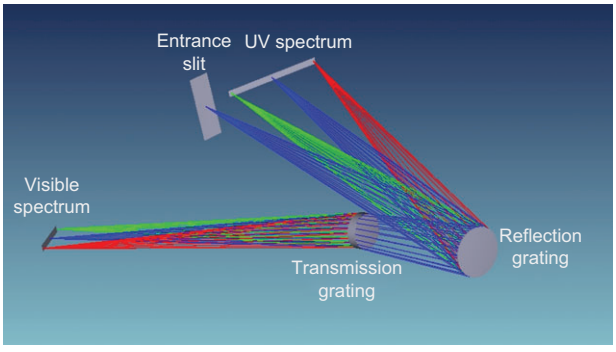

Figure 2 General view of the optical scheme of the dual-band spectrograph.

m	M	λ_{cp}=339 nm y′=0 mm		λ_1=278 nm y′=-13.48 mm		λ_2=400 nm y′=13.84 mm	
		Δy′	Δz′	Δy′	Δz′	Δy′	Δz′
7.8	0	0.015	0	-0.017	0	-0.025	0
5.5	0	0.010	0	-0.012	0	-0.017	0
-5.5	0	-0.011	0	0.015	0	0.011	0
-7.8	0	-0.015	0	0.021	0	0.013	0
0	5.5	-0.004	-0.002	-0.003	-0.146	-0.005	0.171
0	7.8	-0.007	-0.003	-0.005	-0.206	-0.011	0.242

Table 1 Aberrations of the UV channel of the dual-band spectrograph.

The optimal position of the spectrum and coordinates of the recording point sources were determined according to the procedure described in [1]. The calculated distance between the grating vertex and the spectrum center equals 155.3 mm. The angles of incidence of the recording beams onto the grating vertex i_1 and i_2 are 25°10′4″ and -9°39′35″; and the distances from the vertex to the recording point sources d_1 and d_2 are equal to 154.367 mm and 141.053 mm, respectively, for the recording wavelength 441.6 nm.

For the compensation of a residual defocusing on the spectrum edges, a quartz cylindrical concave-plane lens is mounted ahead of the detector plane. The lens meridional radius of curvature is 160 mm, and its axial thickness is 3 mm.

Aberrations of the UV channel of the spectrograph are presented in Table 1. Hereafter, m stands for the meridional coordinate on the entrance pupil of the optical system, M is the corresponding sagittal coordinate; $\Delta y'$ and $\Delta z'$ are the ray aberrations in the meridional and sagittal planes, respectively. The units in the table are in millimeters. Graphs of the instrumental functions for the average and the lateral wavelengths of the working range are plotted in Figure 3. The width of the entrance slit was set to 25 μm in all the calculations. It can be seen from the plots that the spectral resolution, defined as a full width on a half of a maximum (FWHM) of instrument function multiplied by the reciprocal linear dispersion, equals 0.13 nm for the average wavelength and 0.16 nm for the range edges.

4 Optical scheme of visible channel

The working spectral range of the visible channel of the spectrograph is from 400 to 560 nm. A transmission concave holographic grating is used in the second channel. The radius of curvature of the grating surface is 95 mm, and the groove density in its vertex is equal to 700 grooves per mm. The center of the entrance slit image formed by the reflection grating in the zero order of diffraction coincides with the center of curvature of the transmission grating surface. In this case, the grating diameter is 11 mm. The transmission grating operates in a normal incidence scheme in order to decrease the aberrations. The substrate of the grating is made as an achromatic meniscus, thus providing minimization of its influence on the spectrum quality. The radius of curvature of the first surface of the substrate is given by

$$R_1 = R - \frac{1 - \left[n(\lambda_{av})\right]^2}{\left[n(\lambda_{av})\right]^2} t, \tag{18}$$

where $n(\lambda_{av})$ is the refraction index of the substrate material on the average wavelength, t is the axial thickness of the meniscus [11]. For a substrate made of optical glass SCHOTT BK7 (Schott AG, Mainz, Germany) with thickness equal to 3 mm, the first surface radius calculated according to (18) is 96.706 mm.

The length of the spectrum in the second channel is 11.85 mm, which also matches with the dimensions of a commercial detector, for instance Hamamatsu S9037–0902 (Hamamatsu Photonics K.K., Hamamatsu City, Japan) [10].

The coordinates of the spectrum center and the recording point sources were found according to the technique

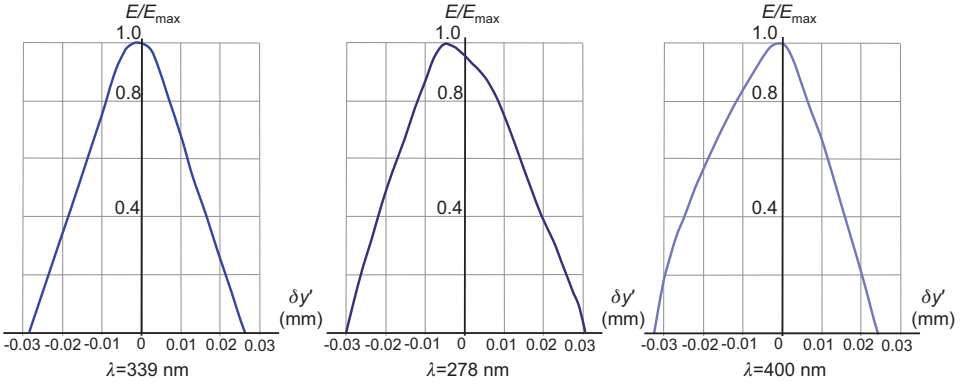

Figure 3 Instrument functions of the UV channel of the dual-band spectrograph.

m	M	λ_{cp}=480 nm y′=0 mm		λ_1=400 nm y′=5.87 mm		λ_2=560 nm y′=-5.99 mm	
		Δy′	Δz′	Δy′	Δz′	Δy′	Δz′
7.8	0	0.007	0	-0.013	0	-0.003	0
5.5	0	0.005	0	-0.008	0	-0.003	0
-5.5	0	-0.005	0	0.005	0	0.008	0
-7.8	0	-0.007	0	0.006	0	0.013	0
0	5.5	0.006	0.004	0.005	-0.023	-0.006	0.031
0	7.8	0.011	0.005	0.009	-0.032	-0.013	0.045

Table 2 Aberrations of the visible channel of the dual-band spectrograph.

described in Section 2. The distance from the transmission grating vertex to the visible spectrum detection plane is 99.49 mm. For the recording wavelength 441.6 nm, the angular coordinates of the recording point sources i_1 and i_2 are 23°21′24″ and 5°0′37″, while the respective linear coordinates d_1 and d_2 are equal to 87.985 mm and 87.603 mm.

As in the previous case, the aberrations of the optical system as well as the instrument functions of the spectrograph were calculated by means of a ray-tracing program. The aberrations are presented in Table 2. Graphs of the

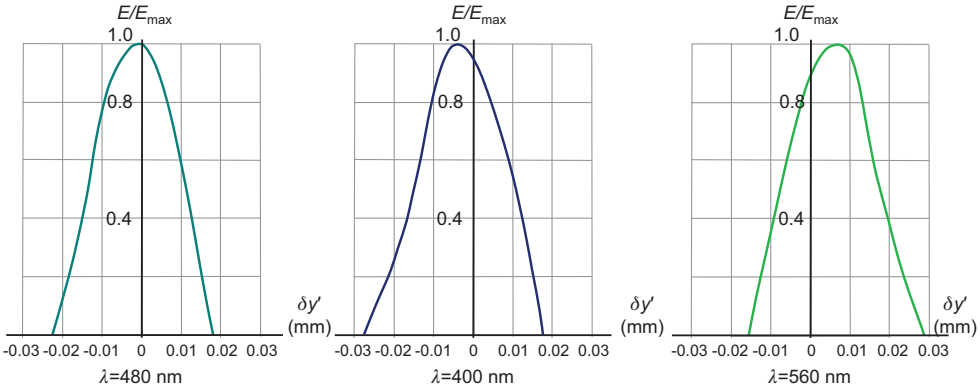

Figure 4 Instrument functions of the visible channel of the dual-band spectrograph.

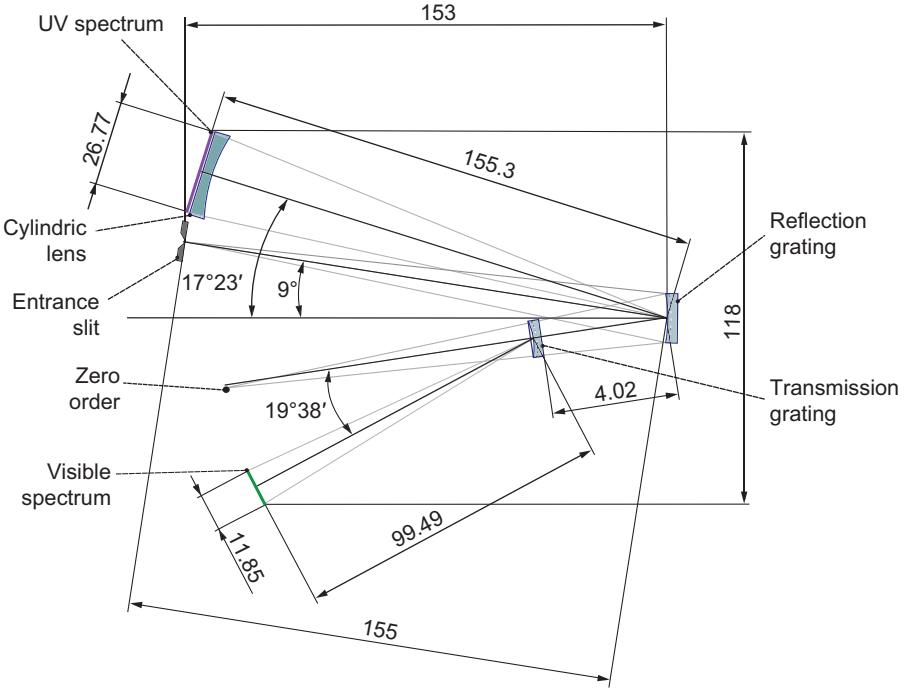

Figure 5 The optical scheme of the dual-band spectrograph.

instrumental functions are depicted in Figure 4. The spectral resolution of the second channel defined through the instrumental function FWHM is 0.34 nm for the center of the working spectral range as well as for its edges.

5 Conclusion

In the present paper, we proposed a concept and design technique of a dual-band spectrograph with a transmission concave holographic grating. The use of the transmission holographic grating mounted in converging beam in the zero order of diffraction of reflection holographic grating makes it possible to detect two spectral subranges simultaneously and provides a relatively high spectral resolution in extended range of wavelengths. In addition, more complete utilization of the radiation is achieved, and overall dimensions of the device do not noticeably increase.

The flat-field spectrograph design procedure is based on the geometrical theory of concave holographic grating. It assures an effective correction of defocusing, astigmatism, and meridional coma on the detection plane.

The developed design method is illustrated on an example of a flat-field spectrograph for near UV-visible range of 278–560 nm. The achieved image quality is proven by the results of computer modeling. The calculated spectral resolution of the spectrometer is 0.16 nm for the UV-subrange and 0.34 nm for the visible subrange.

The resultant layout of the spectrograph optical scheme is presented in Figure 5. The overall size of the scheme does not exceed 153×118×16 mm.

We emphasize the following advantages of our spectrograph: introducing the second channel can significantly increase the dispersion the UV subrange, in which most of the analytical lines are located, without increasing the dimensions of the scheme; the glass substrate of the transmission grating eliminates the spectrum order overlap in the visible channel.

Such instrument can be of great demand for metal and alloy analysis, light source characterization, and other spectroscopic applications.

Thus, we presented a simple method for the increase of the functional capabilities of flat-field spectrographs on the basis of the holographic gratings, and the effectiveness of the used approach is demonstrated as well.

Acknowledgments: The research was supported by Fund for Assistance to Small Innovative Enterprises as a wining project of its 'U.M.N.I.K' grant program in 2011–2012.

Received September 21, 2012; accepted October 5, 2012

References

[1] Zeiss, 'Monolitical Miniature Spectrometer MMS UV', http://www.zeiss.de/c1257682003cbc04/Contents-Frame. Last accessed on 15 Septemer 2012.
[2] Horiba, 'VS140 Low Cost Linear Array Spectrometers', http://www.horiba.com/scientific/products/optical-spectroscopy/. Last accessed on 15 Septemer 2012.
[3] Shimadzu, 'SPECTRO SENSOR OSS-0081', http://www.shimadzu.com/products/opt/ssu.
[4] J. F. Wu, Y. Y. Chen and T. S. Wang, Appl. Opt. 51(4), 59 (2012).
[5] C.-H. Ko and M.-F. Ricky Lee, Opt. Eng. 50(8), 084401 (2011).
[6] L. Poletto and G. Tondello, Proc. SPIE 4138, 182 (2000).
[7] J. T. Meadea, B. B. Behrb and A. R. Hajian, Proc. SPIE 8374, 83740V (2012).
[8] M. N. Nazmeev and N.K. Pavlycheva, Opt. Eng. 33(8), 2777 (1994).
[9] H. Noda, T. Namioka and M. Seya. J. Opt. Soc. Am. 64(8), 1031 (1974).
[10] Hamamtsu, 'CCD Image Sensors', http://sales.hamamatsu.com/en/products/. Last accessed on 15 Septemer 2012.
[11] D. Schroeder, in 'Astronomical Optics', 2nd ed. (Academic Press, San Diego, 2000) pp. 202–203.

Nadezhda K. Pavlycheva is a Professor and Doctor of Technical Sciences. She works at the Department of Optical Electronic Systems, Kazan National Research Technical University. Dr. Pavlycheva's research interests are mainly the investigation and design of optical schemes for spectrographs.

Eduard R. Muslimov received his MSc degree in Optical Technology from the Institute of Automatics and Electronic Instrument Engineering of the Kazan National Research Technical University in 2011. Currently, he is working on his PhD thesis. His scientific work relates to the research of transmission holographic gratings for spectroscopic applications.